ELSEVIER

Thermochimica Acta 366 (2001) 31–36

thermochimica acta

www.elsevier.com/locate/tca

Heat capacity measurements by differential scanning calorimetry in the Pd–Pb, Pd–Sn and Pd–In systems

L. Perring[a,b,1], J.J. Kuntz[b], F. Bussy[c], J.C. Gachon[b,*]

[a]*Institut de Chimie Minérale et Analytique, BCH, Université de Lausanne, CH-1015 Lausanne, Switzerland*
[b]*Laboratoire de Chimie du Solide Minéral, UMR 7555, Groupe Thermodynamique Métallurgique,*
Université Henri Poincaré, Nancy 1, BP 239, F54506 Vandoeuvre-lès-Nancy, Cedex, France
[c]*Institut de Minéralogie et Géochimie, BFSH 2, Université de Lausanne,*
CH-1015 Lausanne, Switzerland

Received 14 March 2000; received in revised form 9 October 2000; accepted 10 October 2000

Abstract

Molar heat capacities at constant pressure of six solid solutions and 11 intermediate phases in the Pd–Pb, Pd–Sn and Pd–In systems were determined each 10 K by differential scanning calorimetry from 310 to 1000 K. The experimental values have been fitted by polynomials $C_p = a + bT + cT^2 + d/T^2$. Results are given, discussed and compared with available literature data. © 2001 Elsevier Science B.V. All rights reserved.

Keywords: Molar heat capacity; Differential scanning calorimetry (DSC); Palladium; Indium; Lead; Tin; Intermetallics

1. Introduction

The knowledge of phase diagrams and thermodynamic properties relative to intermediate phase formation is necessary to understand the chemical bonding and behavior of intermetallics. These quantities are also very useful for the numerical assessments of the multi-element systems. Unfortunately, heat capacities are most often unknown and estimations available in the literature are not accurate enough. This is the reason of this work in our program of experimental determination of intermetallics thermodynamic properties.

We present in this paper our results concerning the molar heat capacities under normal pressure of some Pd–M intermediate compounds and α-Pd(M) solid solutions (with M = In, Pb or Sn). These data have already been used, to compute standard enthalpies of formation at 298.15 K, in combination with Knudsen-cell mass spectrometry (KCMS) results determined at high temperatures and already published [1,2].

Differential scanning calorimetry (DSC) and KCMS had previously been successfully combined in the ruthenium–X systems (with X = Si, Ge and Sn) [3–6].

2. Experimental

Table 1 summarizes the temperatures and types of formation of the phases that were studied.

---

[*] Corresponding author. Fax: +33-3-83-91-2579.
E-mail address: gachon@lcsm.uhp-nancy.fr (J.C. Gachon).
[1] Present address: Nestlé Research Center, Minerals Laboratory, Vers chez les Blanc, CH-1000 Lausanne 26, Switzerland.

PII: S0040-6031(00)00731-0

Table 1
Peritectic and melting temperatures of intermediate phases

	Decomposition T (°C)	Decomposition type	Ref.
Pd_3Pb	1224 ± 3	Congruent	[7]
Pd_3Sn	1340	Congruent	[8]
Pd_2Sn	820	Peritectoid	[9]
PdSn	810	Peritectic	[9]
$PdSn_2$	600	Peritectic	[9]
Pd_3In	1223	Peritectoid	[9]
Pd_2In	1076	Peritectoid	[9]
Pd_5In_3	946	Peritectoid	[9]
PdIn	1285	Congruent	[9]
Pd_2In_3	709	Peritectic	[9]
$PdIn_3$	664	Peritectic	[9]

Table 2
Starting elements characteristics

Elements	Purity (%)	Origin	Shape	Size (mm)
Palladium	99.95	Metalor	Wire	2
Lead	99.9995	Fluka	Bulks	
Tin	99.9995	Balzers	Granulates	2–3
Indium	99.999	Goodfellow	Lumps	5–10

2.1. Preparation of samples and characterization

All palladium alloys were synthesized by induction melting of elements under argon. Table 2 gives element characteristics. After annealing in evacuated silica tubes, alloys were furnace-cooled to room temperature. Powder X-ray diffraction checks were carried out with a Philips PW1370 diffractometer using Cu Kα radiation. Primary solid solutions line shifts compared to pure palladium were controlled as well as mass losses. Chemical compositions of intermediate compounds were obtained by electron probe microanalysis (EPMA) with a Cameca SX50. Pure elements were taken as 100% standards, Lα lines were used, except for Pb which was detected by its Mα radiation. Table 3 shows annealing conditions and EPMA results.

2.2. Differential scanning calorimetry: heat capacity measurements

The heat capacities were determined every 10 K between 310 and 1000 K by a step by step method. Samples with a lower decomposition or melting temperature or being in equilibrium with a liquid–solid two-phase field below 1000 K were studied only up to

Table 3
Annealing conditions and phase composition given by microprobe

Compound (nominal)	Annealing temperature (°C)	Annealing time (days)	Pd (mol.%) (S.D.)	M (mol.%) (S.D.)
1/100 $Pd_{95}Pb_5$	800	20	ND[a]	ND[a]
1/100 $Pd_{90}Pb_{10}$	800	20	ND[a]	ND[a]
14 Pd_3Pb	900	7	74.61 (0.20)	25.39 (0.20)
1/100 $Pd_{95}Sn_5$	800	20	ND[a]	ND[a]
1/100 $Pd_{90}Sn_{10}$	800	20	ND[a]	ND[a]
1/4 Pd_3Sn	900	7	74.92 (0.14)	25.08 (0.14)
1/3 Pd_2Sn	500	14	66.30 (0.28)	33.70 (0.28)
1/2 PdSn	500	14	49.87 (0.20)	50.13 (0.20)
1/3 $PdSn_2$	500	14	33.14 (0.17)	66.86 (0.17)
1/100 $Pd_{95}In_5$	800	20	ND[a]	ND[a]
1/100 $Pd_{90}In_{10}$	800	20	ND[a]	ND[a]
1/4 Pd_3In	900	7	74.22 (0.11)	25.78 (0.11)
1/3 Pd_2In	900	7	66.42 (0.14)	33.58 (0.14)
1/8 Pd_5In_3	900	7	62.40 (0.18)	37.60 (0.18)
1/2 PdIn	900	7	53.46 (0.39)	46.54 (0.39)
1/5 Pd_2In_3	600	14	40.74 (0.22)	59.26 (0.22)
1/4 $PdIn_3$	600	14	30.01 (0.16)	69.99 (0.16)

[a] Not determined.

temperatures which ensured solid state. Measurements were carried out using a Setaram DSC 111, designed as a Calvet type calorimeter with reference and laboratory cells surrounded by two thermal flowmeters connected in opposition. Samples of about 1.5–2.2 g were introduced without crucible (to have the best possible thermal contact and avoid extra heat capacity) in the calorimeter laboratory cell under argon. For each temperature step the heating rate (dT/dt) was 3 K min^{-1} during 200 s ($\Delta T = 10$ K) and then temperature was kept constant during 400 s. This combination gave an overall (dT/dt) of 1 K min^{-1}, which was a compromise between contradictory requirements: (i) the duration of a complete measurement has to be reasonable, (ii) a high (dT/dt) produces sharp signals which are better detected and integrated and (iii) the lower possible (dT/dt) is the one which ensures the smallest departure from equilibrium and which gives the most accurate value for transformation temperatures.

The thermopile signal proportional to the difference of thermal powers exchanged between the laboratory and reference cells and their surroundings was recorded and integrated during the 600 s of the complete sequence. Three temperature runs were necessary, one with the empty laboratory cell, the "blank", one with the calibration material and the last one with the sample. By subtracting the blank signal from both those of calibration material and sample, the results, for each of the individual temperature steps, were proportional to the enthalpy increments $\Delta H_T^{T+\Delta T}$ of the laboratory cell actual content and the proportionality coefficient was given by the calibration material. The C_p mean value on the 10 K step, which can be considered as the value at $T + 5$ K could then be deduced as

$$\overline{C}_p\left(T+\frac{\Delta T}{2}\right)=\frac{\Delta H_T^{T+\Delta T}}{\Delta T}$$

The complete procedure has been described by Cunat and Charles [10] and used in our previous C_ps experimental determinations [5,11]. The calibration material was pure ruthenium, whose heat capacities were first taken from literature [12,13]. Unfortunately, in this compilation experimental C_ps of ruthenium were collected only in two different domains: from 1.2 to 272 K and from 573 to 1877 K. Interpolation led to estimated values between these two temperature ranges. A check of C_p values of Ru against NIST alumina SRM 720 [14] was consequently made to ascertain the Ru values, which we used. No significant differences were found.

No oxidation, appreciable weight losses or reaction between the sample and the calorimeter cell were observed at the end of measurements.

3. Results and discussion

3.1. Accuracy of our results

The reproducibility of the measurements was good (checked by successive runs). The uncertainty of the experimental points was less than 1 J K^{-1} mol^{-1}. The crosscheck of all possible calibrations (Joule effect, alumina SRM 720 [14], comparison to pure metals) shows that an overall uncertainty of ±5% (roughly ±1 J K^{-1} mol^{-1}) is correct.

3.2. Polynomial coefficients

We used the classical form, $C_p = a + bT + cT^2 + d/T^2$ to fit our experimental data. We did not use experimental values below 400 K to compute the parameters because they are more spread than those determined at higher temperatures. Table 4 gives the coefficients a, b, c and d for all the compounds and solid solutions. Figs. 1–8 illustrate the results.

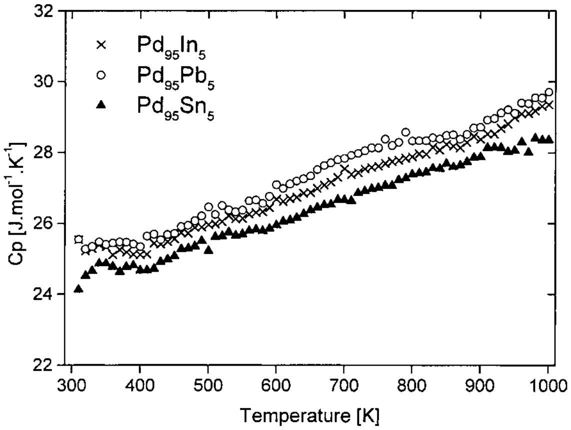

Fig. 1. Experimental C_p of $Pd_{95}Pb_5$ (○), $Pd_{95}Sn_5$ (▲) and $Pd_{95}In_5$ (×).

Table 4
Polynomial coefficients of $C_p = a + bT + cT^2 + d/T^2$ (J K^{-1} mol^{-1})

Phase	Fitting range (K)	a (J K^{-1} mol^{-1})	b (J K^{-1} mol^{-2})	c (J K^{-1} mol^{-3})	d (J K^{-1} mol)
1/100 $Pd_{95}Pb_5$	400–1000	21.80	10.33E-3	−2.64E-6	−18141.5
1/100 $Pd_{90}Pb_{10}$	400–1000	10.38	27.61E-3	−8.97E-6	618433.0
1/4 Pd_3Pb	400–1000	25.48	−3.38E-3	5.58E-6	−179228.3
1/100 $Pd_{95}Sn_5$	400–1000	21.60	8.30E-3	−1.46E-6	4111.0
1/100 $Pd_{90}Sn_{10}$	400–1000	18.41	15.64E-3	−4.37E-6	152959.5
1/4 Pd_3Sn	400–1000	20.46	14.94E-3	−5.04E-6	390878.9
1/3 Pd_2Sn	400–1000	23.32	−6.06E-3	13.50E-6	63316.9
1/2 PdSn	400–820	25.30	−9.58E-3	14.40E-6	−32039.7
1/100 $Pd_{95}In_5$	400–1000	25.34	1.28E-3	2.83E-6	−185925.6
1/100 $Pd_{90}In_{10}$	400–1000	20.55	10.03E-3	−1.39E-6	55660.9
1/4 Pd_3In	400–1000	20.02	3.03E-3	2.22E-6	135222.0
1/3 Pd_2In	400–1000	20.17	8.82E-3	−1.04E-6	171167.7
1/8 Pd_5In_3	400–1000	21.26	52.51E-3	2.39E-6	159869.0
1/2 PdIn	400–1000	18.51	12.59E-3	−3.11E-6	254319.1
1/5 Pd_2In_3	400–920	37.46	−38.01E-3	34.00E-6	−452187.5

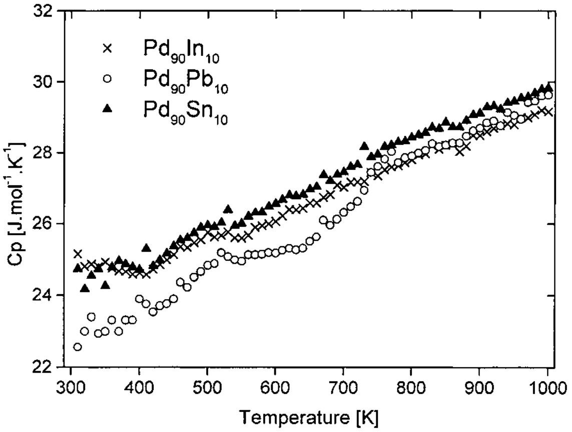

Fig. 2. Experimental C_p of $Pd_{90}Pb_{10}$ (○), $Pd_{90}Sn_{10}$ (▲) and $Pd_{90}In_{10}$ (×).

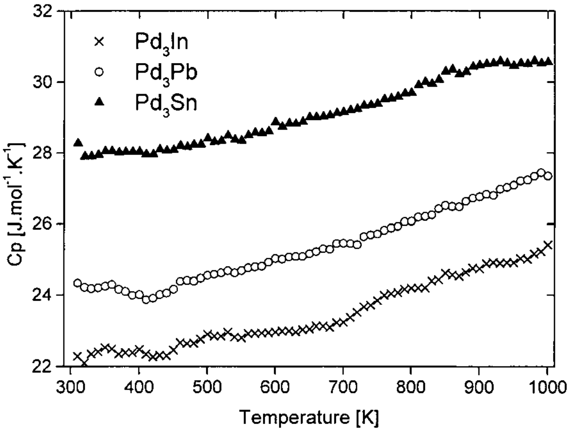

Fig. 3. Experimental C_p of Pd_3Pb (○), Pd_3Sn (▲) and Pd_3In (×).

Table 5
Comparison of our measurements with literature results

Phase	C_p (298 K) in J K^{-1} mol^{-1} (literature)	C_p (298 K) in J K^{-1} mol^{-1} (our results fitting)	Deviation (%)
1/4 Pd_3Sn	24.64 [15]	28.87	−15
1/3 Pd_2Sn	25.23 [15]	23.42	8
1/2 PdSn	25.06 [15]	23.37	7
	24.42 [16]	23.37	4
1/4 Pd_3In	24.70 [17]	22.64	9
1/3 Pd_2In	27.75 [17]	24.63	13
1/2 PdIn	24.70 [17]	24.85	−1
1/5 Pd_2In_3	24.70 [17]	24.06	3

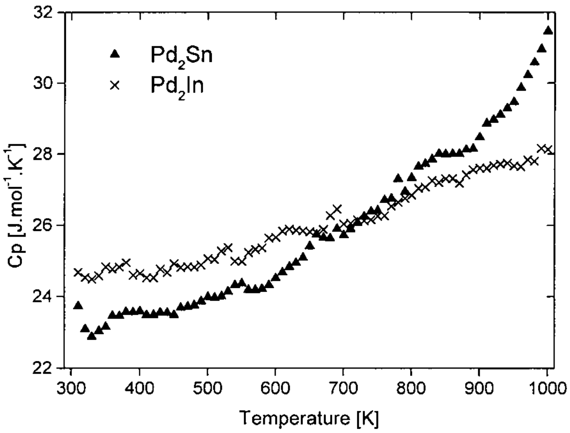

Fig. 4. Experimental C_p of Pd_2Sn (▲) and Pd_2In (×).

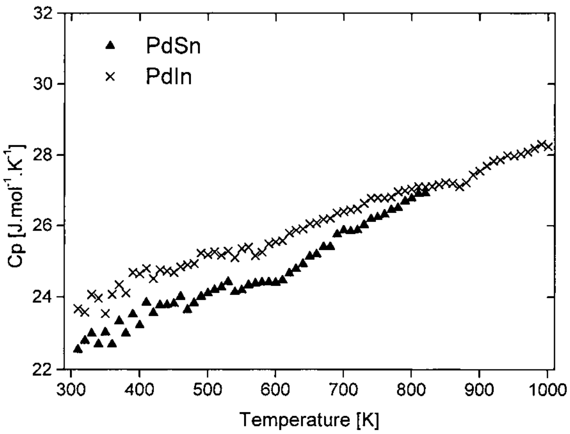

Fig. 5. Experimental C_p of PdSn (▲) and PdIn (×).

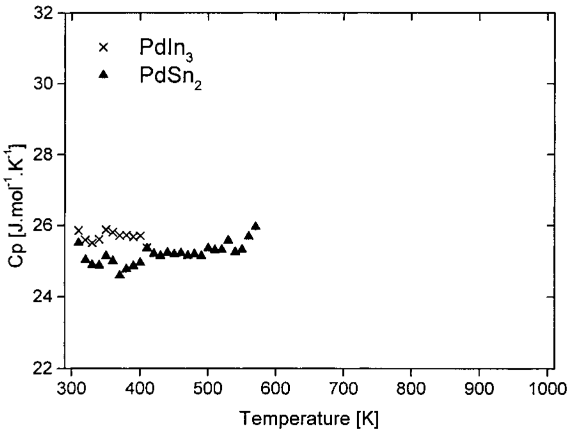

Fig. 6. Experimental C_p of $PdSn_2$ (▲) and $PdIn_3$ (×).

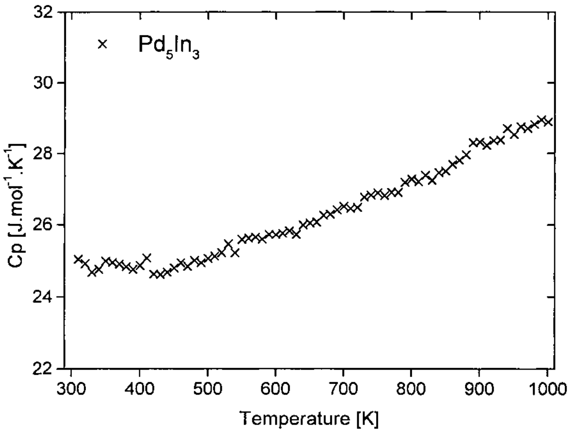

Fig. 7. Experimental C_p of Pd_5In_3 (×).

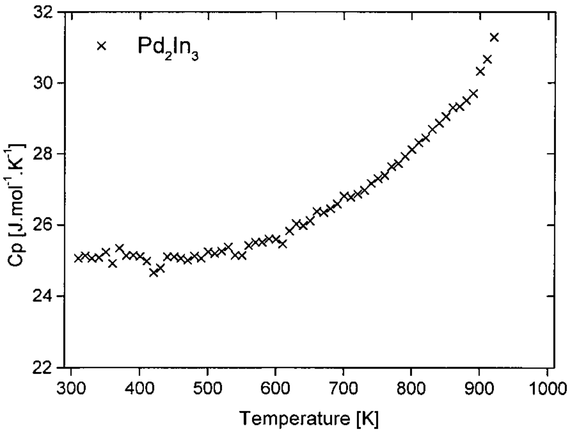

Fig. 8. Experimental C_p of Pd_2In_3 (×).

3.3. Comparison with literature

The comparison between our fitted results and literature data at room temperature is given in Table 5. It can be seen that differences range from 1 to 15%, which underlines that C_p numerical values are not yet well determined, even at room temperature. In addition, the scarcity of data is highlighted, as it is only possible to make a comparison at room temperature.

4. Conclusion

This paper gives new C_p results for 17 different alloys of palladium with indium, tin or lead. The scarcity of data in literature does not allow a throughout comparison and a crosscheck of our work. Our own investigations indicate that the most probable uncertainty of our measurements is about 5% or 1 J K^{-1} mol^{-1}.

Further investigations are necessary to extend the temperature range to higher temperatures and to improve the accuracy of the data.

Suggested Further Reading

S.V. Meschel, O.J. Kleppa, Thermochim. Acta 314 (1998) 205.

R. Lbibb, A. Chouiyakh, R. Castanet, Intermetallics 4 (1996) 589.

V. Vassiliev, G.F. Voronin, G. Borzone, M. Mathon, M. Gambino, J.P. Bros, JALCOM 269 (1998) 123.

A.W. Bryant, W.G. Bugden, J.N. Pratt, Acta Met. 18 (1970) 101.

H.-J. Schaller, H. Brodowsky, Z. Metallkd. 69 (1978) 87.

H.-J. Schaller, H. Brodowsky, Ber. Bunsenges. Phys. Chem. 82 (1978) 773.

W. Bryant, J.N. Pratt, Colloques internationaux du CNRS — Thermochimie 201 (1972) 241.

W. Vogelbein, M. Ellner, B. Predel, Thermochim. Acta 44 (1981) 141.

F.R. de Boer, R. Boom, W.C.M. Mattens, A.R. Miedema, A.K. Niessen, Cohesion in Transition Metals Alloys, North-Holland, Amsterdam, 1988.

References

[1] A. Ciccioli, G. Balducci, G. Gigli, L. Perring, F. Bussy, Intermetallics 5 (2000) 195.

[2] A. Ciccioli, Stabilità termodinamica di sistemi intermetallici: legame e coesione nei sistemi Pd–X, con X appartenente ai gruppi 13 e 14 della tavola periodica, Tesi di dottorato di ricerca in Scienze Chimiche, Università La Sapienza, Roma, Italia, 1999.

[3] L. Perring, J.C. Gachon, J. Alloys Comp. 224 (1995) 228.

[4] L. Perring, P. Feschotte, J.C. Gachon, Thermochim. Acta 293 (1997) 101.

[5] J.J. Kuntz, L. Perring, P. Feschotte, J.C. Gachon, J. Sol. St. Chem. 133 (1997) 439.

[6] A. Ciccioli, G. Balducci, G. Gigli, L. Perring, J.J. Kuntz, J.C. Gachon, Ber. Bunsenges. Phys. Chem. 102 (1998) 1275.

[7] P. Durussel, P. Feschotte, J. Alloys Comp. 236 (1996) 195.

[8] P. Durussel, University of Lausanne-Switzerland, 1998, Private communication.

[9] T.B. Massalski, L.H. Bennett, J.L. Murray, H. Baker, Binary alloy phase diagrams, American Society of Metals International, Metals Park, OH, 1990.

[10] Ch. Cunat, J. Charles, Mem. Scient. Revue de Métallurgie (1982) 177.

[11] L. Perring, J.J. Kuntz, F. Bussy, J.C. Gachon, Intermetallics 7 (1999) 1235.

[12] J. Barin, Thermochemical Data of Pure Substances, third Edition, Part 1 and 2, VCH, Weinheim, Germany, 1995.

[13] R. Hultgren, P.D. Desay, D.T. Hawkins, M. Gleiser, K.K. Kelley, Selected values of the thermodynamic properties of the elements, American Society for Metals, Metals Park, OH, 1973.

[14] D.A. Ditmars, S. Ishihara, S.S. Chang, G. Bernstein, E.D. West, J. Res. NBS 87 (1982) 159.

[15] A.W. Bryant, J.M. Bird, J.N. Pratt, J. Less Common Met. 42 (1975) 249.

[16] M. Mathon, M. Gambino, E. Hayer, M. Gaune-Escard, J.P. Bros, JALCOM 285 (1999) 123.

[17] J.M. Bird, A.W. Bryant, J.N. Pratt, J. Chem. Thermo. 7 (1975) 577.